

# *Lactobacillus brevis* BIOTECH 1766 Attenuates Oxidative Stress and Histopathological Changes following Aluminum Poisoning in ICR Mice

Gerwin Louis T. Dela Torre, RPh,<sup>1</sup> Richelle Ann M. Manalo, RCh, MS,<sup>1,2</sup> Szarina Krisha K. Ko, DVM,<sup>3</sup> Erna C. Arollado, RPh, PhD<sup>1,2</sup> and Arlene A. Samaniego, MD<sup>4</sup>

<sup>1</sup>Institute of Pharmaceutical Sciences, National Institutes of Health, University of the Philippines Manila

<sup>2</sup>Department of Pharmacy, College of Pharmacy, University of the Philippines Manila

<sup>3</sup>Institute of Molecular Biology and Biotechnology, National Institutes of Health, University of the Philippines Manila

<sup>4</sup>Department of Anatomy, College of Medicine, University of the Philippines Manila

## ABSTRACT

**Objective.** The aim of this study was to investigate the protective effects of *Lactobacillus brevis* BIOTECH 1766 against oxidative damage in the brain, liver, and kidneys induced by aluminum (Al) poisoning in ICR mice.

**Methods.** Twenty mice were divided into four groups (n = 5): (I) control, (II) Al, (III) citric acid (CA), and (IV) *L. brevis* BIOTECH 1766 group. A 14-day treatment period was implemented, wherein groups I and II received sterile water, while groups III and IV received 10 mg/kg bw of CA and 1 x 10<sup>9</sup> cfu/kg bw of *L. brevis* BIOTECH 1766, respectively. On day 15, all except the control group received a single oral dose of 1438 mg/kg bw of AlCl<sub>3</sub>·6H<sub>2</sub>O. After 24 h, mice were euthanized to collect the brain, liver, and kidneys for the oxidative stress marker analyses and histopathological examination.

**Results.** Acute intoxication of Al led to a significant increase in tissue malondialdehyde (MDA) and a significant decrease in the tissue's reduced glutathione (GSH), catalase (CAT), and superoxide dismutase (SOD). Mice pretreated with CA or *L. brevis* BIOTECH 1766 have markedly reduced CAT activity in the liver, and SOD in all three organs. Extensive organ injuries were also prevented by CA and *L. brevis* BIOTECH 1766 pretreatment, with the latter providing better protection against liver damage.

**Conclusion.** The findings showed that *L. brevis* BIOTECH 1766 provides a protective effect against acute Al poisoning in mice by ameliorating oxidative damage in the brain, liver, and kidneys.

**Keywords:** aluminum poisoning, catalase, *Lactobacillus brevis*, oxidative stress, superoxide dismutase

## INTRODUCTION

Aluminum (Al) is the third most abundant element existing throughout nature, in air, water, and plants.<sup>1</sup> Aluminum-containing compounds are also used extensively in human products and processes. The most common form of human exposure to Al is through gastrointestinal absorption because salts of Al are used in food additives, pharmaceuticals, and in drinking water purification.<sup>2</sup> In addition, there is the existing issue of food contamination as a result of leaching during the process of food preparation from Al cooking vessels, such as pans and Al foils.<sup>3</sup> Human exposure to Al is therefore difficult to avoid. This is a matter of concern because biologically available Al is highly reactive and essentially toxic.<sup>4</sup> The gastrointestinal absorption and the subsequent accumulation of Al in various organs have



eISSN 2094-9278 (Online)  
Published: October 31, 2024  
<https://doi.org/10.47895/amp.vi0.8005>  
Copyright: The Author(s) 2024

Corresponding author: Gerwin Louis T. Dela Torre, RPh  
Institute of Pharmaceutical Sciences  
National Institutes of Health  
University of the Philippines Manila  
623 Pedro Gil St., Ermita, Manila 1000, Philippines  
Email: gtdelatorre@up.edu.ph  
ORCID: <https://orcid.org/0000-0002-0963-9199>

deleterious health effects.<sup>2</sup> Indeed, epidemiological and experimental studies suggest that Al exposure is linked to brain, liver, and kidney diseases.<sup>5-7</sup>

In Al poisoning cases, deferoxamine has been accepted as one of the preferred treatments.<sup>8</sup> It binds to Al forming aluminoxamine complex which is excreted by the urine.<sup>6</sup> However, aluminoxamine may persist for long periods, especially in kidney diseases causing additional toxicity problems. Further, deferoxamine also has a high affinity with iron, increasing the risk of iron deficiency.<sup>8</sup> Similarly, citric acid (CA) was found to reduce the concentration of Al in acute cases through fecal excretion after binding to the metal.<sup>9</sup> Additionally, CA has been suggested as a prophylactic agent against metal intoxication.<sup>10</sup> Prophylaxis is favored because prevention is far better than treatment of Al poisoning.<sup>11</sup> However, the chronic use of CA may result in liver and kidney damage.<sup>12,13</sup> Thus, the search for prophylactic agents against Al poisoning is warranted.

Lactic acid bacteria (LAB), such as *Lactobacillus brevis*, have been identified as candidate agents in preventing metal toxicity because they have the ability to bind metal ions including mercury, lead, and Al.<sup>14-16</sup> Moreover, they offer an advantage as the majority are generally recognized as safe (GRAS) and are commonly used as probiotics.<sup>17</sup> These microorganisms may produce antioxidant metabolites, and scavenge reactive oxygen species (ROS), which are important in alleviating Al toxicity.<sup>16,18</sup> However, it is important to note, that the bioactivity of microorganisms is strain-specific and cannot be extrapolated to other microbial strains.<sup>19</sup> Thus, assessment of activity must be applied to each candidate strain. In this study, we tested the hypothesis that pretreatment of the BIOTECH 1766 strain of *L. brevis* could alleviate the oxidative damages of acute oral Al poisoning in vivo.

## MATERIALS AND METHODS

### Microbial Strain and Culture

The BIOTECH 1766 strain of *L. brevis* was purchased from the Philippine National Collection of Microorganisms, National Institute of Molecular Biology and Biotechnology, University of the Philippines Los Baños. The microorganism was grown in MRS agar at 37°C for 24 h. Well-isolated colonies were suspended in sterile water and the turbidity was adjusted against a McFarland standard.

### Design of Experiment

Figure 1 presents the experimental process of the study. Twenty, 6-week-old male ICR mice weighing 28-32 g were procured from the Research Institute for Tropical Medicine and were housed in the animal facility of the National Institutes of Health, University of the Philippines Manila. The mice were acclimatized for two weeks. The temperature and humidity were controlled under 12 h light/dark cycles. Animals were fed ad libitum with a standard diet and water. The protocol of the study was approved by the University of the Philippines Manila Institutional Animal Care and Use Committee (Protocol No. 2019-017).

After acclimatization, the mice were randomly assigned to 4 groups (n = 5), namely, (I) control, (II) Al, (III) CA, and (IV) *L. brevis* BIOTECH 1766 group. The comparator used was CA. For 14 days, sterile water was given to mice in groups I and II, while doses of 10 mg/kg bw of CA and  $1 \times 10^9$  cfu/kg bw of *L. brevis* BIOTECH 1766 were given to mice in groups III and IV, respectively.<sup>16,20</sup> On day 15, all mice were given a single oral dose of  $\text{AlCl}_3 \cdot 6\text{H}_2\text{O}$  at a concentration of 1438 mg/kg bw except for mice in group I, wherein sterile water was provided. This dose was found

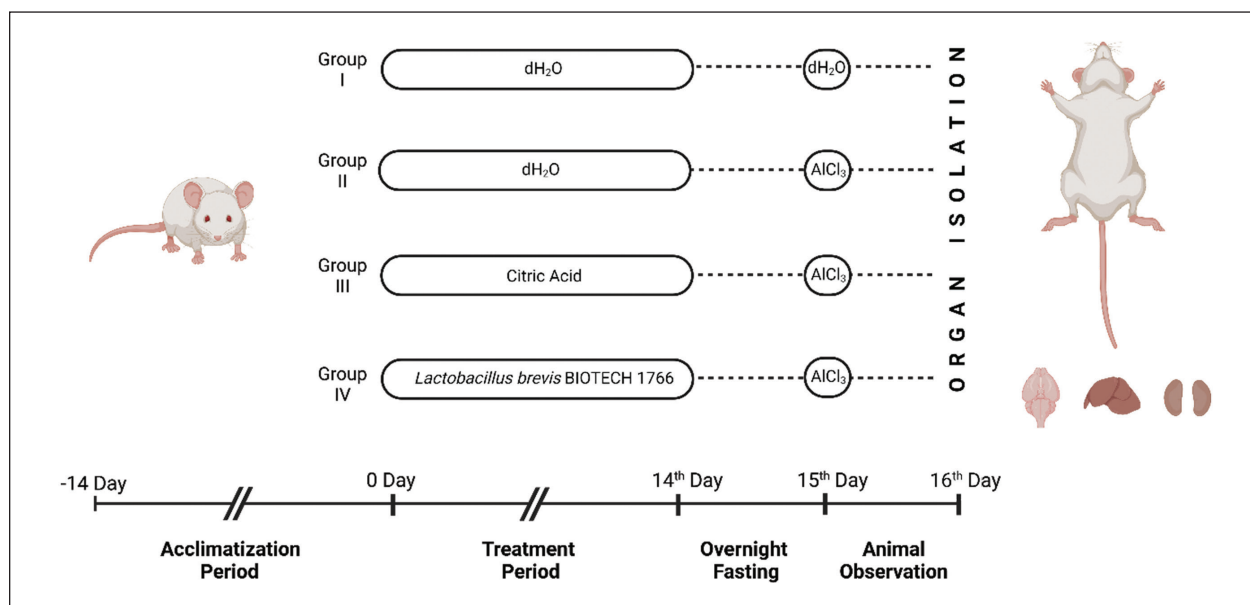


Figure 1. Animal and experimental design (created with BioRender.com).

to induce acute toxicity in mice based on the previous study of Llobet et al.<sup>21</sup> The mice were observed for any signs of toxicity for a period of 24 h. On day 16, all mice were chemically anesthetized with an intraperitoneal injection of tiletamine-zolazepam (Zoletil®; 10 mg/kg bw) prior to euthanasia via decapitation.<sup>22</sup> The brain, liver, and kidneys were excised for the oxidative stress level measurement and histopathological examination.

### Preparation of Tissue Homogenates

The brain, liver, and kidneys were washed with cold saline. Afterward, the organs were homogenized using cold 0.1 mol/L phosphate buffer (pH 7.4). The tissues were minced in a beaker with a pair of sterile surgical scissors. The crude tissue homogenates were centrifugated at 10,000 rpm for 15 min at 4°C and the resulting supernatants were used for the spectrophotometric determination of protein contents, tissue malondialdehyde (MDA), and reduced glutathione (GSH) levels, and tissue superoxide dismutase (SOD) and catalase (CAT) activities.

### Protein Content Determination

The protein contents of the tissues were determined using the Folin-Ciocalteu method. The sample (0.5 mL) was mixed with distilled water (0.10 mL). Alkaline copper solution (3 mL), which consisted of 2% Na<sub>2</sub>CO<sub>3</sub> in 0.1 mol/L NaOH, 0.5% CuSO<sub>4</sub>·5H<sub>2</sub>O, and 1% KNaC<sub>4</sub>H<sub>4</sub>O<sub>6</sub>·4H<sub>2</sub>O, was added followed by vortexing for 30 s. The mixture was then allowed to stand at room temperature for 10 min. Afterward, the Folin-Ciocalteu reagent was added, mixed, and left to stand in the dark for 30 min before reading the absorbance at 600 nm. A standard curve was prepared using bovine serum albumin.<sup>23</sup>

### Tissue MDA Level

Lipid peroxidation in tissue homogenate was measured by estimating the formation of thiobarbituric acid reactive substances (TBARS). The sample (0.2 mL) was mixed with 20% trichloroacetic acid (1 mL) and 1.34% thiobarbituric acid (1 mL). The volume was made to 3 mL using distilled water, vortexed for 10 s, and heated at 95°C for 20 min. The mixture was cooled, followed by the addition of n-butanol (3 mL). Subsequently, the mixture was centrifugated at 10,000 rpm for 5 min, and the supernatant's absorbance was measured at 532 nm against a reagent blank. The TBARS as MDA content of the sample was calculated using the molar extinction coefficient value of  $1.56 \times 10^5$  L/mol per cm and expressed as nmol/mg protein.<sup>24,25</sup>

### Tissue GSH Level

The determination of GSH level followed the method of Jollow et al.<sup>26</sup> The sample (1 mL) was mixed with 4% sulfosalicylic acid (1 mL). The mixture was incubated at 4°C for 1 h and centrifugated at 10,000 rpm for 15 min. The resulting supernatant (0.2 mL) was mixed with 0.1

mol/L phosphate buffer, pH 7.4 (2.6 mL), and 5,5'-dithio-bis(2-nitrobenzoic acid) at a concentration of 4 mg/mL in 0.1 mol/L phosphate buffer, pH 7.4 (0.2 mL). The mixture was vortexed for 10 s, after which the absorbance was read at 412 nm against a reagent blank. The GSH was calculated using the molar extinction coefficient of  $1.3 \times 10^4$  L/mol per cm and was expressed as nmol/mg protein.

### Tissue CAT Activity

The CAT activity was measured using the method of Hadwan with some modifications.<sup>27</sup> The sample (0.5 mL) and 10 mmol/L H<sub>2</sub>O<sub>2</sub> (1 mL) were mixed and incubated at 37°C for 2 min. Afterward, a working solution (6 mL) was added which contains Co<sup>2+</sup>, Na(PO<sub>3</sub>)<sub>6</sub>, and NaHCO<sub>3</sub> solutions. The mixture was vortexed for 5 s and was kept in the dark at room temperature for 10 min. The changes in absorbance were recorded at 440 nm against a reagent blank. A standard solution was also prepared composed of distilled water, 10 mmol/L H<sub>2</sub>O<sub>2</sub>, and the working solution. The CAT activity was expressed as U/mg protein.

### Tissue SOD Activity

The SOD activity in the tissue was measured using the SOD assay kit (Sigma-Aldrich 19160) which was performed according to the recommendation of the manufacturer.<sup>28</sup> The tissue SOD activity was expressed as U/mg protein.

### Histopathological Examination

The excised brain, liver, and kidneys were fixed with a 10% formalin solution. The tissues were embedded in paraffin and sectioned at 5 µm thickness. Sections were stained with hematoxylin-eosin (H&E) for light microscopy examination. The results of the histopathological examination were semi-statistically evaluated.<sup>29,30</sup>

The list of changes in the brain tissues that were observed includes the vacuolization around the neuron or perinuclear space, disruption or degeneration of neurons, neurofibrillary tangles, neuronal cytoplasm shrinkage, and plaque formation; for liver tissues, the changes include the loss of intact liver plates, chromatin condensation, cytoplasmic vacuolization, and necrosis of hepatocytes; and for kidney tissues, the changes include the loss of intact tubules and glomeruli, dilation in the glomeruli, and tubular necrosis.

### Statistical Analyses

Statistical analyses were performed using Statistical Package for the Social Sciences (SPSS) 23.0. Results were reported as mean ± standard deviation (SD). Data were checked for normality and homogeneity of variance using Shapiro-Wilk and Levene's tests, respectively. Depending on the results, data were analyzed with one-way analysis of variance (ANOVA) followed by Tukey's post hoc test or Kruskal-Wallis test followed by Dunn's multiple comparison test. Values of p<0.01 were considered statistically significant.

## RESULTS

### Acute AI Toxicity

No mortality was observed in any of the groups up to the end of the animal experiment. However, the administration of a single oral dose of  $\text{AlCl}_3 \cdot 6\text{H}_2\text{O}$  on day 15 caused observable signs of toxicity in the 24 h observation period, in the form of decreased locomotor activity, lethargy, and piloerection. These signs were observed in all mice of the AI group, while only three mice experienced the signs in both the CA and *L. brevis* BIOTECH 1766 groups.

### Oxidative Stress Markers Estimation

Table 1 summarizes the estimated oxidative stress markers in the brain, liver, and kidneys of mice. In the AI

group, the MDA levels were higher except in the liver, and the GSH levels were lower in all organs when compared to other groups, but the differences did not reach statistically significant values ( $p > 0.01$ ). No significant differences were also identified among the groups in the brain and kidney CAT activities ( $p > 0.01$ ). Interestingly, pretreatment of CA and *L. brevis* BIOTECH 1766 was effective in increasing the CAT activity in the liver and the SOD activities in all organs ( $p < 0.01$ ). However, when compared to CA, *L. brevis* BIOTECH 1766 had statistically lower SOD activities in the liver ( $p = 0.005$ ) and kidney ( $p < 0.001$ ).

### Histopathological Findings

Scores of histopathological changes are summarized in Table 2. Representative brain tissue photomicrographs

**Table 1.** Effects of Different Treatments on the Levels of MDA and GSH, and the CAT and SOD Activities in the Brain, Liver, and Kidneys of Mice

Group	MDA level (nmol/mg protein)	GSH level (nmol/mg protein)	CAT activity (U/mg protein)	SOD activity (U/mg protein)
<b>Brain</b>				
Control	250.94±23.47	10.87±2.13	116.34±0.49	91.89±1.91 <sup>bc</sup>
AI	284.48±24.67	0.58±0.30	19.06±0.40	10.52±0.20 <sup>ac</sup>
CA	250.91±47.11	3.39±1.17	63.99±0.52	51.43±3.87 <sup>ab</sup>
<i>L. brevis</i> BIOTECH 1766	233.72±65.38	2.90±1.28	41.07±0.61	49.05±1.36 <sup>ab</sup>
<b>Liver</b>				
Control	187.48±58.03	1.20±0.19	129.94±3.96 <sup>bc</sup>	6.95±0.23 <sup>b</sup>
AI	232.71±27.14	0.28±0.13	51.85±0.99 <sup>ac</sup>	4.58±0.07 <sup>ac</sup>
CA	254.67±15.79	0.63±0.18	85.90±2.44 <sup>ab</sup>	6.84±0.16 <sup>b</sup>
<i>L. brevis</i> BIOTECH 1766	189.02±51.25	0.47±0.16	80.84±1.27 <sup>ab</sup>	6.17±0.17 <sup>abc</sup>
<b>Kidney</b>				
Control	142.86±38.33	1.50±0.59	148.37±0.81	18.86±0.24 <sup>bc</sup>
AI	246.91±74.14	0.20±1.10	113.20±0.31	13.97±0.13 <sup>ac</sup>
CA	208.85±28.68	0.67±0.88	118.49±0.17	16.89±0.43 <sup>ab</sup>
<i>L. brevis</i> BIOTECH 1766	144.44±54.65	0.71±0.01	115.33±0.23	15.11±0.23 <sup>abc</sup>

Values expressed as mean ± SD. Per organ, the superscripts a, b, and c indicate statistically significant differences compared to the control, AI, and CA group, respectively at  $p < 0.01$ .

**Table 2.** Histopathological Scores of the Brain, Liver, and Kidney Tissues per Treatment Group, Based on the Indicated Signs

Tissue	Indicated sign	Score of groups			
		Control	AI	CA	<i>L. brevis</i> BIOTECH 1766
<b>Brain</b>	Vacuolization around the neuron or perinuclear space	-	-	-	-
	Disruption or degeneration of neurons	-	++	+	+
	Neurofibrillary tangles	-	++	+	+
	Shrunken cytoplasm of the neuron	-	+	+	+
	Presence of plaques	-	-	-	-
<b>Liver</b>	Loss of intact liver plates	-	++	+	-
	Chromatin condensation	-	++	+	+
	Cytoplasmic vacuolization	-	-	-	-
	Necrosis of hepatocytes	-	++	+	-
<b>Kidneys</b>	Loss of intact tubules and glomeruli	-	+	-	-
	Dilation in the glomeruli	-	-	-	-
	Tubular necrosis	-	+	-	-

(-) No change observed in the samples; (+) Changes rarely observed in the samples with an average of 1-2 changes per vision field; (++) Changes occasionally observed in the samples with an average of 8-10 changes per vision field; (+++) Changes often observed in the sample with >20 changes per vision field.

of mice from each group are depicted in Figure 2. The brain tissue of mice in the control group appeared normal. Histopathological changes were observed for the Al, CA, and *L. brevis* BIOTECH 1766 groups. In the Al group, mononuclear cell infiltrations, granulovacuolar changes, and basophilic necrotic neurons were seen. It was also noted that mononuclear cell infiltrations were found in the CA group, while neuronal disruptions occurred in the *L. brevis* BIOTECH 1766 group. Figure 3 shows the representative hepatic photomicrographs of mice in each group. Liver sections of mice in the control group were found to be normal, while several other histopathological anomalies were identified in other groups. In the Al group, centrilobular degeneration, focal loss of intact hepatic cords, sinusoidal dilatation, and focal perivascular infiltration of mononuclear cells were identified. In the CA group, perivascular inflammation and karyolysis were apparent, while in the *L. brevis* BIOTECH 1766 group, small inflammatory cell aggregates were seen.

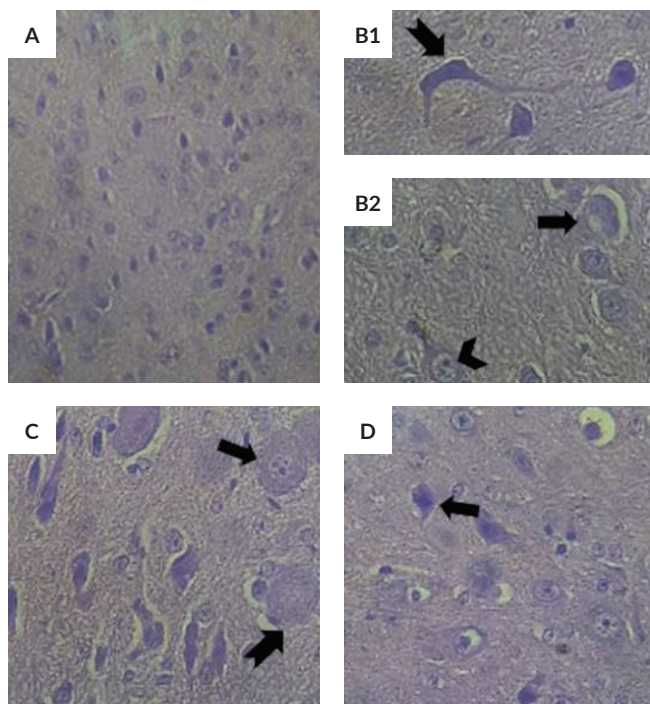


**Figure 2.** Representative photomicrographs of brain tissue of mice (H&E stain; 100x magnification). (A) Brain tissue of mice in the control group with normal histology; (B) brain tissue of mice in Al group with [1] irregularly shaped darkly staining neurons with neurofibrillary tangles (notched arrow), [2] central chromatolysis (full-bodied arrow) and enlarged astrocytes (arrowhead); (C) brain tissue of mice in CA group showing granulovacuolar changes (full-bodied arrow), and neuronal central chromatolysis (notched arrow); and (D) brain tissue of mice in *L. brevis* BIOTECH 1766 group showing basophilic irregularly shaped shrunken neurons (full-bodied arrow).

Lastly, representative renal photomicrographs of each group are shown in Figure 4. Normal histological structures were evident in the kidneys of mice in the control, CA, and *L. brevis* BIOTECH 1766 groups. In the Al group, focal tubular degenerations were visible.

## DISCUSSION

Earlier studies have shown that Al compounds are capable of inducing acute toxicity with high doses.<sup>21,31</sup> The results of our present study clearly confirmed that a single oral dose of  $\text{AlCl}_3 \cdot 6\text{H}_2\text{O}$  at a concentration of 1438 mg/kg bw caused distress in mice. On the basis of ion, the concentration is equivalent to 161 mg Al/kg bw. Observed reduced locomotor activity, lethargy, and piloerection are all attributable signs of acute Al toxicity and possible organ injuries.<sup>21</sup> In our study, these physical signs were visually observed to be present in all mice of Al group. For both the CA and *L. brevis* BIOTECH 1766 groups, the absence of the physical signs was noted on two mice, which is indicative of the protective effect of the pretreatment.

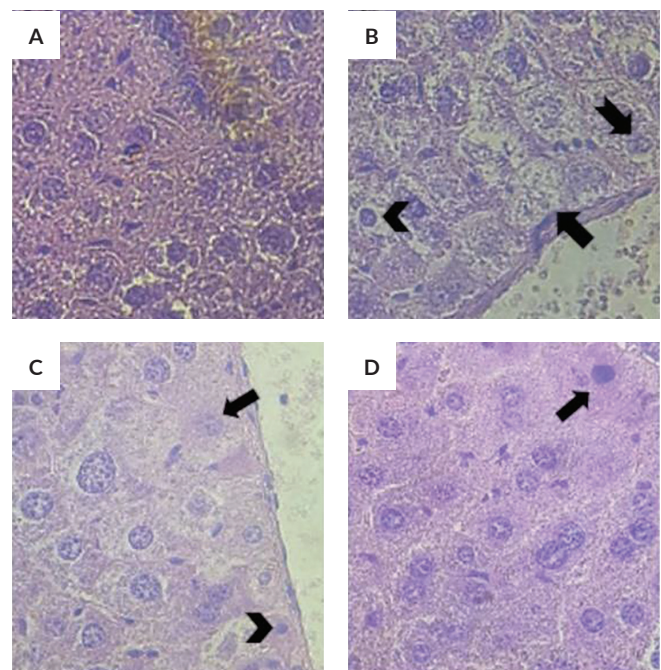


**Figure 3.** Representative photomicrographs of liver tissue of mice (H&E stain; 400x magnification). (A) Normal liver tissue of mice in the control group; (B) liver tissue of mice in Al group depicting centrilobular degeneration, with karyopyknosis (arrowhead), karyolysis (full-bodied arrow), and karyorrhexis (notched arrow); (C) liver tissue of mice in CA group showing centrilobular degeneration with karyorrhexis (full-bodied arrow) and karyopyknosis (arrowhead); and (D) liver tissue of mice in *L. brevis* BIOTECH 1766 group with karyopyknosis (full-bodied arrow).

It is a fact that high levels of Al accumulating in the organs can lead to toxic effects.<sup>32</sup> Hence, preventing Al from reaching the organs is an avenue to avert tissue damage. One of the binding agents, effective in removing Al in biological systems is CA.<sup>9</sup> However, the excessive use of CA carries its own ill health effects.<sup>12,13</sup> Thus, there was a proposed shift in the use of the members of LAB, possessing both antioxidant and metal binding activity as an intervention to prevent metal toxicity, such as that of Al. However, the present study only focused on the evaluation of the antioxidant property of *L. brevis* BIOTECH 1766 in terms of oxidative stress modulation.

It is known that Al causes oxidative stress in the brain, liver, and kidney tissues.<sup>33</sup> High MDA levels, which are the end product of the lipid peroxidation process, can serve as a reliable marker of oxidative stress. In addition, drastic amounts of ROS exhaust GSH, CAT, and SOD, leaving no protection against tissue damage.<sup>29,34</sup> These were evident in the Al group when compared against the other groups, wherein MDA levels were highest in brain and kidneys, while GSH, CAT, and SOD were lowest in the brain, liver, and kidneys of mice following the acute Al poisoning. The findings indicate that the antioxidant defense grid was impaired. Statistically

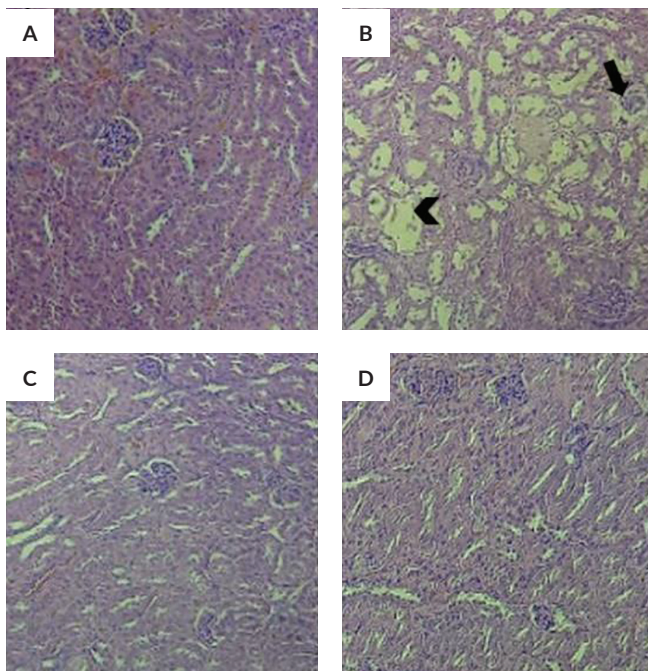


**Figure 4.** Representative photomicrographs of kidney tissue of mice (H&E stain; 400x magnification). (A) Kidney tissue of mice in the control group with normal structures; (B) kidney tissue of mice in Al group showing diffused tubular degradation, loss of intact glomerulus (full-bodied arrow) and tubule (arrowhead); (C) kidney tissue of mice in CA group showing normal features; and (D) normal kidney tissue of mice in *L. brevis* BIOTECH 1766 group.

significant improvements in the oxidative stress markers were observed among mice pretreated with CA and *L. brevis* BIOTECH 1766, specifically the CAT activity in the liver, and SOD activity in all three organs. The protection provided by *L. brevis* BIOTECH 1766 against oxidative damage was consistent with previous reports using different strains of *L. brevis*. Noureen et al. demonstrated that administration of *L. brevis* MG000874 improved SOD and CAT activities in the brain, liver, and kidneys of mice subjected to a murine model of oxidative stress. Furthermore, the strain upregulated both SOD and CAT expression.<sup>35,36</sup> Although our study found that the administration of LAB caused an insignificant improvement in MDA and GSH, other scientists reported otherwise. Han et al. showed the protective effect of *L. brevis* HY7401 on tert-butylperoxide-induced liver injury in mice by decreasing the MDA levels.<sup>37</sup> Jiang et al. concluded that *L. brevis* 23017 relieves mercury toxicity by modulating oxidative stress which includes reducing MDA levels and increasing the activity of GSH.<sup>14</sup> These differences may be attributed to the strains, doses, and experimental designs used. Regardless of the differences, these bioactivities may be partly related to the antioxidant and other metabolites with intrinsic antioxidant activity that *L. brevis* produces.

Histopathologically, we found that pretreatment of *L. brevis* BIOTECH 1766 minimized brain, liver, and kidney injuries. It performed better than the CA in preventing histopathological changes in the liver. The protection can be ascribed to the previously reported metal-binding trait of *L. brevis*.<sup>14-16</sup> The present study did not quantify both the capacity of the BIOTECH 1766 strain to bind Al as well as the amount of deposited Al in the organs after pretreatment. These, however, must be clarified in future research to better understand the protective effect of *L. brevis* BIOTECH 1766. In general, Al is absorbed in the intestines finding its way to the systemic circulation wherein it can be transported to different organs.<sup>38</sup> Findings from the histopathological analysis showed that acute oral exposure to Al caused substantial alteration in the brain, liver, and kidney structures. Looking at the brain, the toxicity of Al affects biological reactions such as axonal transport, neurotransmitter synthesis, synaptic transmission, and protein degradation.<sup>39</sup> In the present study, degeneration of neurons and neurofibrillary tangles were observed in the brain tissue of mice in Al group. A link between Al and the appearance of neurofibrillary degeneration and of neurofibrillary tangle-like structures in the brain has been established previously.<sup>40,41</sup> Neurofibrillary tangles are formed in the cytoplasmic regions where Al accumulates amongst aggregates of hyperphosphorylated tau.<sup>42</sup> These abnormalities diminished in occurrence and became rare on mice pretreated with CA and *L. brevis* BIOTECH 1766. Moreover, our study demonstrated granulovacuolar degeneration and necrosis in the brain of mice in Al group, as a response to the oxidative stress induced by Al.<sup>42</sup> Except for the control group, infrequent shrinkage of the cytoplasm and darkening of neurons were likewise observed. These have been reported

before in the brain of rats intoxicated with  $AlCl_3$ .<sup>30</sup> In the CA and *L. brevis* BIOTECH 1766 groups, basophilic or dark neurons, and white matter vacuolation were observed. However, these alterations are common artefactual findings in the rodent brain, especially in non-perfused tissues related to the prolonged fixation process.<sup>43</sup> Hence, it is imperative to determine if Al poisoning is related to these changes in future research. Liver toxicity is also a manifestation of excessive Al exposure. It was reported that Al causes liver dysfunction due to mitochondrial oxidative damage. Specifically,  $AlCl_3$  exposure causes hepatocellular destruction and necrosis.<sup>44</sup> In our histopathological finding, occasional necrosis of hepatocytes, chromatin condensation, and loss of intact liver plates were observed in the liver tissues of mice in Al group. These observations concurred with studies on the hepatotoxicity of Al.<sup>16,45</sup> Results of CA pretreatment reduced chromatin condensation and hepatic necrosis, while *L. brevis* BIOTECH 1766 pretreatment prevented the loss of intact liver plates and necrosis of hepatocytes. Lastly, the kidneys are also vulnerable to Al-mediated toxicity. This is due to the fact that the primary route of elimination for Al is through urine, thus kidneys are exposed to Al in the normal process of renal excretion. Diffused tubular necrosis and the loss of intact glomeruli and tubules in the Al group of our study were identified which were in line with previous Al toxicity reports.<sup>46,47</sup> Interference in glomerular hemodynamics might have occurred that resulted in the morphological changes.<sup>48</sup> The CA and *L. brevis* BIOTECH 1766 groups revealed no apparent renal histopathological changes, similar to the normal histological architecture of the control. Although the present study did not evaluate the effects of *L. brevis* BIOTECH 1766 on the inflammatory response, prior studies involving different *L. brevis* strains concluded that the reduction of pro-inflammatory factors helped in alleviating pathological changes,<sup>14,49</sup> and this mechanism can be investigated in future studies involving the BIOTECH 1766 strain.

## CONCLUSION

The present study revealed that pretreatment of *L. brevis* BIOTECH 1766 in mice offered protection against Al poisoning by attenuating oxidative stress, specifically improving the activities of CAT in the liver and SOD in all three organs. Extensive histopathological injuries were likewise prevented by the microbial strain. Given this knowledge, *L. brevis* BIOTECH 1766 can be considered a potential agent in preventing Al-induced damage in the brain, liver, and kidneys. This work also calls for further studies on other protective mechanisms of *L. brevis* BIOTECH 1766 against Al poisoning.

## Statement of Authorship

All authors certified fulfillment of ICMJE authorship criteria.

## Author Disclosure

All authors declared no conflicts of interest.

## Funding Source

The study was funded by the National Institutes of Health, University of the Philippines Manila (NIH: 2018-012).

## REFERENCES

- Kumar V, Gill KD. Aluminium neurotoxicity: neurobehavioural and oxidative aspects. *Arch Toxicol.* 2009 Nov;83(11):965-78. doi: 10.1007/s00204-009-0455-6. PMID: 19568732.
- Bondy SC. The neurotoxicity of environmental aluminum is still an issue. *Neurotoxicology.* 2010 Sep;31(5):575-81. doi: 10.1016/j.neuro.2010.05.009. PMID: 20553758; PMCID: PMC2946821.
- Liukkonen-Lilja H, Piepponen S. Leaching of aluminium from aluminium dishes and packages. *Food Addit Contam.* 1992 May-Jun; 9(3):213-23. doi: 10.1080/02652039209374065. PMID: 1397396.
- Exley C. The toxicity of aluminium in humans. *Morphologie.* 2016 Jun;100(329):51-5. doi: 10.1016/j.morpho.2015.12.003. PMID: 26922890.
- Kawachi I, Pearce N. Aluminium in the drinking water-is it safe? *Aust J Public Health.* 1991 Jun;15(2):84-7. doi: 10.1111/j.1753-6405.1991.tb00316.x. PMID: 1912063.
- Rahimzadeh MR, Rahimzadeh MR, Kazemi S, Amiri RJ, Pirzadeh M, Moghadamnia AA. Aluminum poisoning with emphasis on its mechanism and treatment of intoxication. *Emerg Med Int.* 2022 Jan;2022:1480553. doi: 10.1155/2022/1480553. PMID: 35070453; PMCID: PMC8767391.
- Bondy SC. Prolonged exposure to low levels of aluminum leads to changes associated with brain aging and neurodegeneration. *Toxicology.* 2014 Jan;315:1-7. doi: 10.1016/j.tox.2013.10.008. PMID: 24189189.
- Smith SW. The role of chelation in the treatment of other metal poisoning. *J Med Toxicol.* 2013 Dec;9(4):355-69. doi: 10.1007/s13181-013-0343-6. PMID: 24113858; PMCID: PMC3846962.
- Domingo JL, Gomez M, Llobet JM, Corbella J. Comparative effects of several chelating agents on the toxicity, distribution and excretion of aluminium. *Hum Toxicol.* 1988 May;7(3):259-62. doi: 10.1177/096032718800700305. PMID: 3391623.
- Lawrence GD, Patel KS, Nusbaum A. Uranium toxicity and chelation therapy. *Pure Appl Chem.* 2014 Apr;86(7):1105-10. doi: 10.1515/pac-2014-0109.
- Levine S, Malone E, Lekiachvili A, Briss P. Health care industry insights: why the use of preventive services is still low. *Prev Chronic Dis.* 2019 Mar;16:E30. doi: 10.5888/pcd16.180625. PMID: 30873937; PMCID: PMC6429690.
- Aktac T, Kaboglu A, Ertan F, Ekinci F, Huseyinova G. The effects of citric acid (antioxidant) and benzoic acid (antimicrobial agent) on the mouse liver: biochemical and histopathological study. *Biologia.* 2003 May;58(3):343-7.
- Chen X, Lv Q, Liu Y, Deng W. Effects of the food additive, citric acid, on kidney cells of mice. *Biotech Histochem.* 2015 Jan;90(1):38-44. doi: 10.3109/10520295.2014.937745. PMID: 25196033.
- Jiang X, Gu S, Liu D, Zhao L, Xia S, He X, et al. *Lactobacillus brevis* 23017 relieves mercury toxicity in the colon by modulation of oxidative stress and inflammation through the interplay of MAPK and NF- $\kappa$ B signaling cascades. *Front Microbiol.* 2018 Oct;9:2425. doi: 10.3389/fmicb.2018.02425. PMID: 30369917; PMCID: PMC6194351.
- Dai QH, Bian XY, Li R, Jiang CB, Ge JM, Li BL, et al. Biosorption of lead(II) from aqueous solution by lactic acid bacteria. *Water Sci Technol.* 2019 Feb;79(4):627-34. doi: 10.2166/wst.2019.082. PMID: 30975929.

16. Yu L, Zhai Q, Liu X, Wang G, Zhang Q, Zhao J, et al. *Lactobacillus plantarum* CCFM639 alleviates aluminium toxicity. *Appl Microbiol Biotechnol*. 2016 Feb;100(4):1891-900. doi: 10.1007/s00253-015-7135-7. PMID: 26618083.
17. Min KH, Yin FH, Amin Z, Mansa RF, Ling CMWV. An overview of the role of lactic acid bacteria in fermented foods and their potential probiotic properties. *BIJB*. 2022 Dec;2(2022):65-83. doi: 10.51200/bijb.v2i.4186.
18. Wang Y, Wu Y, Wang Y, Xu H, Mei X, Yu D, et al. Antioxidant properties of probiotic bacteria. *Nutrients*. 2017 May;9(5):521. doi: 10.3390/nu9050521. PMID: 28534820; PMCID: PMC5452251.
19. Fijan S. Microorganisms with claimed probiotic properties: an overview of recent literature. *Int J Environ Res Public Health*. 2014 May;11(5):4745-67. doi: 10.3390/ijerph110504745. PMID: 24859749; PMCID: PMC4053917.
20. Chen L, Li M, Wu JL, Li JX, Ma ZC. Effect of lemon water soluble extract on hyperuricemia in a mouse model. *Food Funct*. 2019 Sep;10(9):6000-8. doi: 10.1039/C9FO00509A. PMID: 31482168.
21. Lobet JM, Domingo JL, Gomez M, Tomas JM, Corbella J. Acute toxicity studies of aluminium compounds: antidotal efficacy of several chelating agents. *Pharmacol Toxicol*. 1987 Apr;60(4):280-3. doi: 10.1111/j.1600-0773.1987.tb01752.x. PMID: 3588526.
22. Lee YO, Shin JW, Yi C, Lee YH, Sohn NW, Kang C, et al. Detection of A $\beta$  plaques in mouse brain by using a disaggregation-induced fluorescence-enhancing probe. *Chem Commun*. 2014 Jun;50(43):5741-4. doi: 10.1039/c4cc02011a. PMID: 24752243.
23. Rodger A, Sanders K. UV-visible absorption spectroscopy, biomacromolecular applications. In: Lindon JC, Tranter GE, Koppenaal DW, eds. *Encyclopedia of spectroscopy and spectrometry*, 3rd ed. United Kingdom: Elsevier; 2017. pp. 495-502.
24. Dassarma B, Nandi DK, Gangopadhyay S, Samanta S. Hepatoprotective effect of food preservatives (butylated hydroxyanisole, butylated hydroxytoluene) on carbon tetrachloride-induced hepatotoxicity in rat. *Toxicol Rep*. 2017 Nov;5:31-7. doi: 10.1016/j.toxrep.2017.12.009. PMID: 29276688; PMCID: PMC5730417.
25. Nogaïm QA, Bugata LSP, Pv P, Reddy UA, Gowri P M, Kumari S I, et al. Protective effect of Yemeni green coffee powder against the oxidative stress induced by ochratoxin A. *Toxicol Rep*. 2020 Jan;7:142-8. doi: 10.1016/j.toxrep.2019.11.015. PMID: 31956515; PMCID: PMC6962656.
26. Jollow DJ, Mitchell JR, Zampaglione N, Gillette JR. Bromobenzene-induced liver necrosis. Protective role of glutathione and evidence for 3,4-bromobenzene oxide as the hepatotoxic metabolite. *Pharmacology*. 1974;11(3):151-69. doi: 10.1159/000136485. PMID: 4831804.
27. Hadwan MH. Simple spectrophotometric assay for measuring catalase activity in biological tissues. *BMC Biochem*. 2018 Aug;19(1):7. doi: 10.1186/s12858-018-0097-5. PMID: 30075706; PMCID: PMC6091033.
28. Liu T, Xiao B, Xiang F, Tan J, Chen Z, Zhang X, et al. Ultrasmall copper-based nanoparticles for reactive oxygen species scavenging and alleviation of inflammation related diseases. *Nat Commun*. 2020 Jun;11(1):2788. doi: 10.1038/s41467-020-16544-7. PMID: 32493916; PMCID: PMC7270130.
29. Zhai Q, Wang G, Zhao J, Liu X, Tian F, Zhang H, et al. Protective effects of *Lactobacillus plantarum* CCFM8610 against acute cadmium toxicity in mice. *Appl Environ Microbiol*. 2013 Mar;79(5):1508-15. doi: 10.1128/AEM.03417-12. PMID: 23263961; PMCID: PMC3591948.
30. Liaquat L, Sadir S, Batool Z, Tabassum S, Shahzad S, Afzal A, et al. Acute aluminum chloride toxicity revisited: study on DNA damage and histopathological, biochemical and neurochemical alterations in rat brain. *Life Sci*. 2019 Jan;217:202-11. doi: 10.016/j.lfs.2018.12.009. PMID: 30528774.
31. Kumar S. Acute toxicity of aluminium chloride, acephate, and their coexposure in male Wistar rat. *Int J Toxicol*. 2001 Jul-Aug;20(4):219-23. doi: 10.1080/109158101750408046. PMID: 11563417.
32. Ohtman MS, Obeidat ST, Aleid GM, Al-Bagawi AH, Fehaid A, Habotta OA, et al. Protective effect of Allium atroviolaceum-synthesized SeNPs on aluminium-induced brain damage in mice. *Open Chem*. 2022 Nov;20(1):1365-77. doi: 10.1515/chem-2022-0245.
33. Wen YF, Zhao JQ, Nirala SK, Bhadauria M. Aluminum-induced toxicity and its response to combined treatment of HEDTA and propolis in rats. *Pol J Environ Stud*. 2012;21(5):1437-43.
34. Ighodaro OM, Akinloye OA. First line defence antioxidants-superoxide dismutase (SOD), catalase (CAT) and glutathione peroxidase (GPX): their fundamental role in the entire antioxidant defence grid. *Alexandria J Med*. 2018 Dec;54(4):287-93. doi: 10.1016/j.ajme.2017.09.001.
35. Noureen S, Riaz A, Arshad M, Arshad N. In vitro selection and in vivo confirmation of the antioxidant ability of *Lactobacillus brevis* MG000874. *J Appl Microbiol*. 2019 Apr;126(4):1221-32. doi: 10.1111/jam.14189. PMID: 30597726.
36. Noureen S, Liaquat I, Riaz A, Rana M, Arshad N. Evaluation of *Lactobacillus brevis* MG000874 in behavioral and in vitro antioxidant enzyme activity of murine brain. *Braz Arch Biol Technol*. 2022 May;65:e22210294. doi: 10.1590/1678-4324-2022210294.
37. Han SY, Huh CS, Ahn YT, Lim KS, Baek YJ, Kim DH. Hepatoprotective effect of lactic acid bacteria. *J Microbiol Biotechnol*. 2005 Aug;15(4):887-90.
38. Igbokwe IO, Igwenagu E, Igbokwe NA. Aluminium toxicosis: a review of toxic actions and effects. *Interdiscip Toxicol*. 2019 Oct;12(2):45-70. doi: 10.2478/intox-2019-0007. PMID: 32206026; PMCID: PMC7071840.
39. Kawahara M, Kato-Negishi M. Link between aluminum and the pathogenesis of Alzheimer's disease: the integration of the aluminum and amyloid cascade hypotheses. *Int J Alzheimers Dis*. 2011 Mar;2011:276393. doi: 10.4061/2011/276393. PMID: 21423554; PMCID: PMC3056430.
40. Klatzo I, Wisniewski H, Streicher E. Experimental production of neurofibrillary degeneration. I. Light microscopic observations. *J Neuropathol Exp Neurol*. 1965 Apr;24:187-99. doi: 10.1097/00005072-196504000-00002. PMID: 14280496.
41. Crapper DR, Krishnan SS, Dalton AJ. Brain aluminum distribution in Alzheimer's disease and experimental neurofibrillary degeneration. *Science*. 1973 May;180(4085):511-3. doi: 10.1126/science.180.4085.511. PMID: 4735595.
42. Walton JR. An aluminum-based rat model for Alzheimer's disease exhibits oxidative damage, inhibition of PP2A activity, hyperphosphorylated tau, and granulovacuolar degeneration. *J Inorg Biochem*. 2007 Sep;101(9):1275-84. doi: 10.1016/j.jinorgbio.2007.06.001. PMID: 17662457.
43. Garman RH. Artifacts in routinely immersion fixed nervous tissue. *Toxicol Pathol*. 1990;18(1 Pt 2):149-53. doi: 10.1177/019262339001800120. PMID: 2195635.
44. El-Demerdash FM. Antioxidant effect of vitamin E and selenium on lipid peroxidation, enzyme activities and biochemical parameters in rats exposed to aluminium. *J Trace Elem Med Biol*. 2004;18(1):113-21. doi: 10.1016/j.jtemb.2004.04.001. PMID: 15487771.
45. Teschke R. Aluminum, arsenic, beryllium, cadmium, chromium, cobalt, copper, iron, lead, mercury, molybdenum, nickel, platinum, thallium, titanium, vanadium, and zinc: molecular aspects in experimental liver injury. *Int J Mol Sci*. 2022 Oct;23(20):12213. doi: 10.3390/ijms232012213. PMID: 36293069; PMCID: PMC9602583.
46. Al Dera HS. Protective effect of resveratrol against aluminum chloride induced nephrotoxicity in rats. *Saudi Med J*. 2016 Apr;37(4):369-78. doi: 10.15537/smj.2016.4.13611. PMID: 27052279; PMCID: PMC4852014.
47. Abdel-Hamid GA. Effect of vitamin E and selenium against aluminum-induced nephrotoxicity in pregnant rats. *Folia Histochem Cytobiol*. 2013;51(4):312-9. doi: 10.5603/FHC.2013.0042. PMID: 24497136.
48. Al Kahtani MA. Renal damage mediated by oxidative stress in mice treated with aluminum chloride: protective effects of taurine. *J Biol Sci*. 2010;10(7):584-95. doi: 10.3923/jbs.2010.584.595.
49. Han X, Ding S, Ma Y, Fang J, Jiang H, Li Y, et al. *Lactobacillus plantarum* and *Lactobacillus brevis* alleviate intestinal inflammation and microbial disorder induced by ETEC in a murine model. *Oxid Med Cell Longev*. 2021 Sep;2021:6867962. doi: 10.1155/2021/6867962. PMID: 34594475; PMCID: PMC8478549.